Research article

NMR IN BIOMEDICINE

Received: 16 October 2014, Revised: 22 January 2015, Accepted: 23 January 2015, Published online in Wiley Online Library

(wileyonlinelibrary.com) DOI: 10.1002/nbm.3276

Single-shot single-voxel lactate measurements using FOCI-LASER and a multiple-quantum filter

Geoffrey S. Payne*, Nandita M. deSouza, Christina Messiou and Martin O. Leach

Measurement of tissue lactate using ^{1}H MRS is often confounded by overlap with intense lipid signals at 1.3 ppm. Single-voxel localization using PRESS is also compromised by the large chemical shift displacement between voxels for the 4.1 ppm (–CH) resonance and the 1.3 ppm –CH_3 resonance, leading to subvoxels with signals of opposite phase and hence partial signal cancellation. To reduce the chemical shift displacement to negligible proportions, a modified semi-LASER sequence was written ("FOCI-LASER", abbreviated as fLASER) using FOCI pulses to permit high RF bandwidth even with the limited RF amplitude characteristic of clinical MRI scanners. A further modification, MQF-fLASER, includes a selective multiple-quantum filter to detect lactate and reject lipid signals.

The sequences were implemented on a Philips 3 T Achieva TX system. In a solution of brain metabolites fLASER lactate signals were 2.7 times those of PRESS. MQF-fLASER lactate was 47% of fLASER (the theoretical maximum is 50%) but still larger than PRESS lactate. In oil, the main 1.3 ppm lipid peak was suppressed to less than 1%. Enhanced suppression was possible using increased gradient durations. The minimum detectable lactate concentration was approximately 0.5 mM. Coherence selection gradients needed to be at the magic angle to avoid large water signals derived from intermolecular multiple-quantum coherences. In pilot patient measurements, lactate peaks were often observed in brain tumours, but not in cervix tumours; lipids were effectively suppressed.

In summary, compared with PRESS, the fLASER sequence yields greatly superior sensitivity for direct detection of lactate (and equivalent sensitivity for other metabolites), while the single-voxel single-shot MQF-fLASER sequence surpasses PRESS for lactate detection while eliminating substantial signals from lipids. This sequence will increase the potential for *in vivo* lactate measurement as a biomarker in targeted anti-cancer treatments as well as in measurements of tissue hypoxia. Copyright © 2015 John Wiley & Sons, Ltd.

Keywords: Spectroscopic localization; MR Spectroscopy (MRS) and Spectroscopic Imaging (MRSI) Methods; lactate, multiple quantum filter, FOCI; LASER; brain

INTRODUCTION

Lactate is potentially an important biomarker of tissue hypoxia and for tumour evaluation and response. While normal tissue concentrations of lactate are low, varying between about 0.1 mM in the fully fasted state and about 1.5 mM following a high-carbohydrate meal, blood concentrations may rise to 6 mM during exercise (1). Tissue concentrations are elevated in many tumours, including brain (2,3), prostate (4), and squamous cell carcinoma (5).

Elevated lactate concentration in tumours is predominantly a consequence of the Warburg effect, in which tumour cells undergo glycolysis even in the presence of oxygen. Sometimes lactate accumulation is enhanced by low perfusion, reducing wash-out of the lactate produced. Preclinical and clinical studies have shown that elevated tumour lactate concentrations can also be associated with subsequent development of nodal and distant metastatic disease (6–10). Tumour lactate concentrations are affected directly or indirectly by several chemotherapeutic agents (11) and mechanism-based anticancer drugs, such as phosphoinositide 3-kinase inhibitors (12), dichloroacetate (13), and Mek inhibitors (14). Inhibitors of mono-carboxylate transporters (15) would also be expected to affect tumour lactate concentrations.

Measuring lactate using ^{1}H MRS in tumours *in vivo* is hampered by the spectral overlap with lipids (see below). This is particularly a problem outside the brain or close to the skull. Most reported studies have been in brain tumours, where lipids tend to be relatively low, motion is limited, and lactate is present at concentrations of up to 14 mM (3,16–19). Lactate tends to be higher in high-grade tumours and in metastases (3). A study in paediatric diffuse brainstem gliomas showed that response to treatment was associated with a reduction in lactate

* *Correspondence to: G. S. Payne, Cancer Research UK Cancer Imaging Centre, Royal Marsden Hospital and Institute of Cancer Research, Sutton, Surrey, UK. E-mail: gsp@icr.ac.uk*

G. S. Payne, N. M. deSouza, C. Messiou, M. O. Leach
Cancer Research UK Cancer Imaging Centre, Royal Marsden Hospital and Institute of Cancer Research, Sutton, Surrey, UK

Abbreviations used: *FOCI, frequency offset corrected inversion; LASER, localization by adiabatic selective refocusing; fLASER, LASER using FOCI pulses; MQF, multiple-quantum filter; PRESS, point resolved spectroscopy; SAR, specific absorption rate.*

concentration, whilst no change was detected in non-responders (19). Lactate concentration has also been found to depend on the degree of oxygenation: healthy subjects breathing 12% O_2 exhibited a 39% increase in brain lactate compared with breathing 21% O_2 (20). Outside the brain, pilot measurements have detected lactate in non-Hodgkin lymphoma (21), but in prostate tumours the concentration of lactate has been found to be below the threshold for detection (22).

Lactate is an AX_3 spin system characterized by a $–CH_3$ doublet peak at 1.33 ppm and a –CH quartet at 4.1 ppm, with a *J*-coupling constant of 6.9 Hz. The 1.33 ppm doublet is the preferred resonance for measurement since it is larger, narrower, and not affected by water suppression pulses at 4.7 ppm. One difficulty in measurement is that lactate suffers from the chemical shift displacement artefact, which causes the slices selected by excitation and refocusing pulses during volume selection to be spatially shifted for the –CH quartet at 4.1 ppm relative to the $–CH_3$ doublet at 1.3 ppm. In the point resolved spectroscopy (PRESS) sequence for example this leads to some sub-volumes of the total voxel experiencing only one or zero 180° refocusing RF pulses of the coupled spins, affecting phase evolution and leading to opposing phase in these regions and therefore overall partial signal cancellation (23). This effect can be mitigated by expanding the nominal voxel size and then using saturation slices to eliminate the unwanted signals (24) or improved broadband RF pulse design (25).

Measurement of the 1.3 ppm peak using ^{1}H MRS is confounded in many cases by intense overlapping signals from lipids. Many options have been proposed to selectively detect lactate signals in these cases, most exploiting the *J*-coupling between the $–CH_3$ and the –CH resonances, although the relatively long T_2 of lactate compared with lipid has also been used (26). The lactate resonance also overlaps with a smaller macromolecule resonance, which also needs to be taken into account (20).

For applications *in vivo* the criteria to be considered include good elimination of lipid signals, good retention of lactate signals, good tolerance to motion, and capability to localize to the tissue of interest.

Employing *long echo times* to favour lactate detection over lipid is simple but insufficient to eliminate the strong lipid signals often found in tumours. In *spin-echo difference editing*, selective 180° RF pulses at the frequency of the 4.1 ppm methine spins are applied during alternate scans, which affect the phase evolution of the 1.3 ppm lactate doublet of interest; subtracting these scans causes signals from lactate to add and from singlets to cancel (27–29). However, small tissue motion leads to incomplete subtraction of the large lipid signals. This makes the method possible for measurements in the head (17,30), but not where motion is present.

Multiple-quantum filters (MQFs) separate single-quantum coherences of non-coupled metabolites from multiple-quantum coherences of coupled spins (e.g. lactate) using phase-cycling or gradient pulses. Using gradient pulses for coherence selection permits lactate editing in a single shot, but in the basic implementation loses 75% of the signal. Strategies have been suggested to increase MQF lactate signals, with up to 100% lactate signal recovery in an unlocalized single acquisition demonstrated on a high-field preclinical system (31). However, on clinical systems the best that has been reported to date is 50% in a single acquisition, or 100% using a phase cycle (32). In general, the initial excitation pulse can be made slice selective without affecting coherence pathways, while MRSI can be achieved by including appropriate phase encoding. Originally implemented on a high-field animal scanner, a more recent publication has extended the MRSI localization to multi-slice using Hadamard encoding on a clinical scanner, and has demonstrated this in a non-Hodgkin lymphoma (21). A single-slice version has demonstrated ability to detect lactate in the presence of otherwise-dominant lipid resonances in patients with high-grade glioma (33).

While MRSI methods have good coverage, they are subject to errors in the presence of motion, and have relatively large minimum acquisition times owing to the number of phase encode steps involved. An option for single-voxel localization for lactate is therefore desirable. Unfortunately, incorporating an MQF into a PRESS sequence does not work, owing to the chemical shift displacement artefact (34).

The aim of the present work therefore was to develop and evaluate a single-shot single-voxel measurement of tumour lactate as a potential non-invasive imaging biomarker of disease and response. The strategy was firstly to modify a semi-LASER (localization by adiabatic selective refocusing) sequence, by replacing the hyperbolic secant RF pulses with FOCI (frequency offset corrected inversion) RF and gradient pulses. FOCI pulses produce very sharp slice profiles with high RF bandwidth, but unlike hyperbolic secant pulses do not require a high RF amplitude (35,36) and are therefore compatible with standard clinical MRI systems. They should largely eliminate the chemical shift displacement problem. A similar strategy has been reported for single-voxel localization (37), MRSI (38), and MEGA editing (39) in brain, and for MRSI in prostate (40,41). An MQF module was then inserted in the centre of this sequence to selectively detect lactate signals while suppressing signals from the 1.3 ppm resonance of lipids. The implementation of this method is described, together with evaluation in test objects and a pilot cohort of patients with brain and cervical tumours *in vivo*.

METHODS

Semi-LASER sequences comprise slice-selective excitation followed by two pairs of identical adiabatic inversion RF pulses (usually hyperbolic secant) with appropriate slice-select and spoiler gradients (6). Unfortunately, the maximum pulse amplitude permitted by the hardware limits the maximum achievable spectral bandwidth; on our 3 T Philips Achieva TX system the maximum available B_1 on the body coil (13.5 μT) limits the maximum hyperbolic secant pulse bandwidth to about 1200 Hz, resulting in poor slice profiles and a 1/3 voxel shift between lactate CH and CH_3. We therefore implemented 12 kHz FOCI RF-and-gradient pulses to replace them (indicated in brown and maroon in Fig. 1). We will refer to semi-LASER with FOCI pulses as "FOCI-LASER" (abbreviated fLASER).

The MQF-fLASER sequence (Fig. 1) was created by additionally inserting an MQF segment (based on that of Mellon *et al*. (21)) at $T_E/2$. Originally, we used similar RF pulses to Mellon *et al*. for this, using 6 ms sinc-gauss frequency-selective 90° and 180° RF pulses, with the 90° pulses centred at the frequency of water and lactate –CH and the 180° pulse offset by 434 Hz (lactate $–CH_3$). The purpose of using frequency-selective RF pulses for this was to affect one group of lactate spins but not the coupled partners, and hence reduce the contribution of lipid (which has no coupled spins at 4.1 ppm). We found that rectangular pulses with appropriate durations (2.714 ms for 90° and 2.408 ms for 180°) worked at least as well in the MQF-fLASER sequence as the

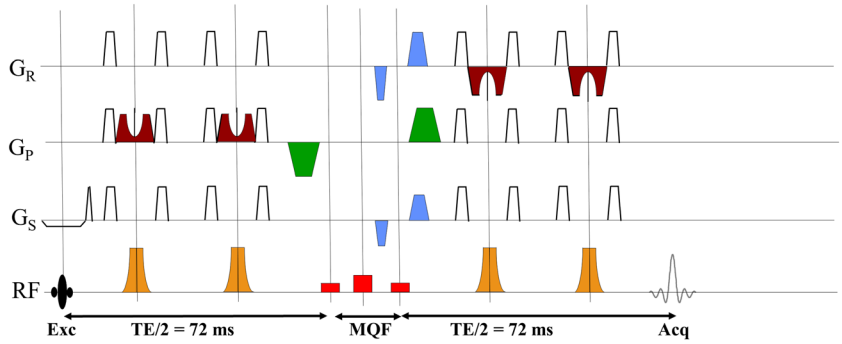

Figure 1. MQF-fLASER sequence timing diagram. The initial slice-selective excitation is followed by a pair of FOCI combined RF (brown) and gradient (maroon) refocus pulses. The MQF is positioned at $T_E/2$, comprising rectangular 90°–180°–90° RF pulses (shown in red) and coherence selection gradients in the ratio −1:2 at the magic angle (shown in blue). Additional crusher gradients (shown in green) are positioned around the MQF segment. A further pair of slice-selective FOCI pulses is followed by acquisition.

sinc-gauss pulses and also enabled us to reduce the total mixing time, which can be a significant source of signal loss (32). It was also found that for the MQF-fLASER sequence (but not for a 2D MRSI MQF sequence such as that of Mellon *et al.*) centring all three pulses at −90Hz on the lactate –CH resonance improved signal detection. Coherence selection gradients (shown in blue) in the ratio −1:2 were placed before and after the second rectangular 90° pulse of the MQF. These were at the magic angle (54.7° to *z*) to avoid refocusing intermolecular multiple quantum coherences from water (42). A further pair of spoiler gradients was placed around the MQF period along *y* (green), which needed to have the same polarity when the MQF refocus pulse was centred at the frequency of the lactate $–CH_3$, and opposite polarity when the MQF refocus pulse was at the frequency of the lactate –CH resonance.

Measurements were made on a 3 T Philips Achieva TX MRI system (Best, The Netherlands). Phantom measurements used the eight-channel SENSE Head coil. The fLASER and MQF-fLASER sequences were compared with the standard PRESS sequence (RF bandwidth 1200 Hz) in a 15 cm diameter spherical phantom of brain metabolites, including 5 mM lactate, and in a 50 ml tube of safflower oil. All phantom measurements were acquired with voxel size (2 cm)^3, Number of signal averages (NSA) = 128, T_R = 1000 ms, T_E = 144 ms, 2048 sampling points over a 4 kHz bandwidth. All scans were acquired using "frequency stabilization", which measures and corrects the water frequency before each acquisition to offset effects of scanner drift during the scan. This made a significant improvement to data quality. Lactate signal intensity in the phantoms was measured both using peak amplitude (after zero-filling twice, and apodizing with a 1 Hz line broadening), and the Quest algorithm in jMRUI (43–45).

Pilot data using the fLASER and MQF-fLASER sequences were acquired from seven patients with brain tumours (six glioblastomas, one meningioma, voxel sizes 8–15 cm^3) and seven patients with cervical cancers (voxel sizes 3.8–15.6 cm^3) within a protocol approved by our institutional review board. fLASER spectra without water suppression were also acquired to enable the use of tissue water as a concentration reference. Brain scans were acquired using the eight-channel SENSE Head coil while scans on cervical cancer patients were acquired using combined external loop coils (diameter = 20 cm) and an internal coil (46) to improve signal to noise ratio. In addition one patient was scanned with a breast lesion (using the standard breast coil, and voxel size (2 cm)^3, primarily to explore the degree of fat suppression provided by the MQF-fLASER sequence *in vivo*), and large voxels (6 cm × 4 cm × 4 cm) were studied in the brains of two normal volunteers (to investigate whether significant signals are passed by the MQF from macromolecules at about 1.3 ppm coupled to others at about 4.3 ppm (47).

RESULTS

Phantom studies

A comparison of the standard PRESS, fLASER and MQF-fLASER spectra from the sphere of brain metabolites is shown in Fig. 2 (a). The standard PRESS sequence shows all metabolites, but lactate signal is low owing to the chemical shift displacement effect, which creates subvoxels of lactate with signals of opposite phase to each other, which then cancel (26). This effect was much reduced with the fLASER sequence, with a corresponding large increase (×2.7) in detected lactate signal. The MQF-fLASER eliminated singlets but retained significant signal from lactate. Using the lactate signal of the fLASER signal as a reference, the MQF-fLASER sequence yielded 47 ± 1% lactate signal (based on peak area; 46 ± 1% based on peak height, N = 5), while the PRESS signal yielded 37 ± 5 % lactate signal (based on peak area; 38 ± 1% based on peak height, N = 5). Thus the MQF-fLASER lactate signals were close to the theoretical maximum of 50% (48,31), and were about 20% larger than the standard PRESS lactate signals. Some signal is also seen from the coupled spins in glutamate, but these do not interfere with the lactate signals. The lactate signal-to-noise ratio (peak signal/peak–peak noise) in the MQF-fLASER spectrum is approximately 10:1, meaning that with this hardware and these sequence parameters (2 cm cubic voxel, 2 min acquisition) the lowest detectable lactate concentration is approximately 0.5 mM.

The MQF-fLASER spectrum of the oil phantom (Fig. 2(b)) shows signal at 1.3 ppm of 0.86% relative to the amplitude of this peak in the fLASER spectrum, demonstrating good lipid suppression. Signal from the 2 ppm allyl peak was detected as expected (21).

In vivo studies

Example fLASER and MQF-fLASER spectra from brain tumours are shown in Fig. 3. In both cases the fLASER spectra show large peaks at 1.3 ppm, which must be primarily from lipid since they

NMR IN BIOMEDICINE

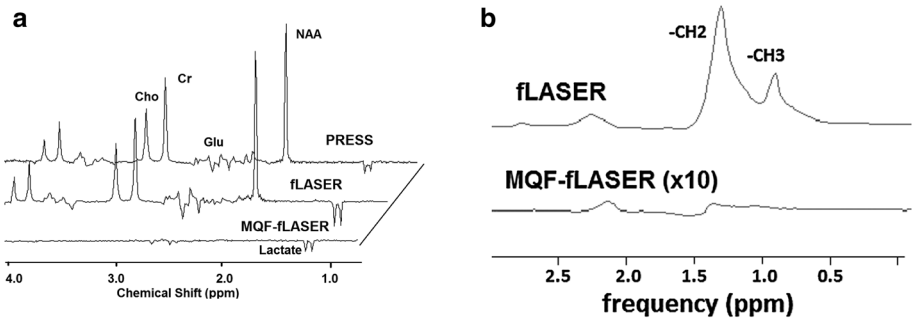

Figure 2. (a) PRESS, fLASER and MQF-fLASER spectra from solution of brain metabolites (12.5 mM N-acetyl aspartate (NAA), 10 mM creatine (Cr), 3 mM choline (Cho), 7.5 mM myo-inositol, 12.5 mM glutamate (Glu), 5 mM lactate). $(2\ cm)^3$ voxel, 128 acquisitions, T_R 1000 ms, T_E 144 ms. Data were zero filled from 2048 to 4096 points, and apodized with 1 Hz line broadening. Note that while the amplitudes of the singlets (e.g. creatine) are similar in PRESS and fLASER spectra, the lactate signal is substantially larger in the fLASER spectrum as it does not suffer significant signal loss from the chemical shift displacement artefact effect. In these spectra the MQF-fLASER lactate peak is 46% of that in the fLASER (i.e. nearly the theoretical maximum), and is also larger than that in the PRESS spectrum. (b) fLASER and MQF-fLASER spectra of safflower oil. $(2\ cm)^3$ voxel, T_R = 1000 ms, T_E = 144 ms, NSA = 128 (fLASER) and 256 (MQF-fLASER). The MQF-fLASER spectrum is displayed after a ×10 vertical expansion. Note the almost total suppression of the lipid resonance at 1.3 ppm.

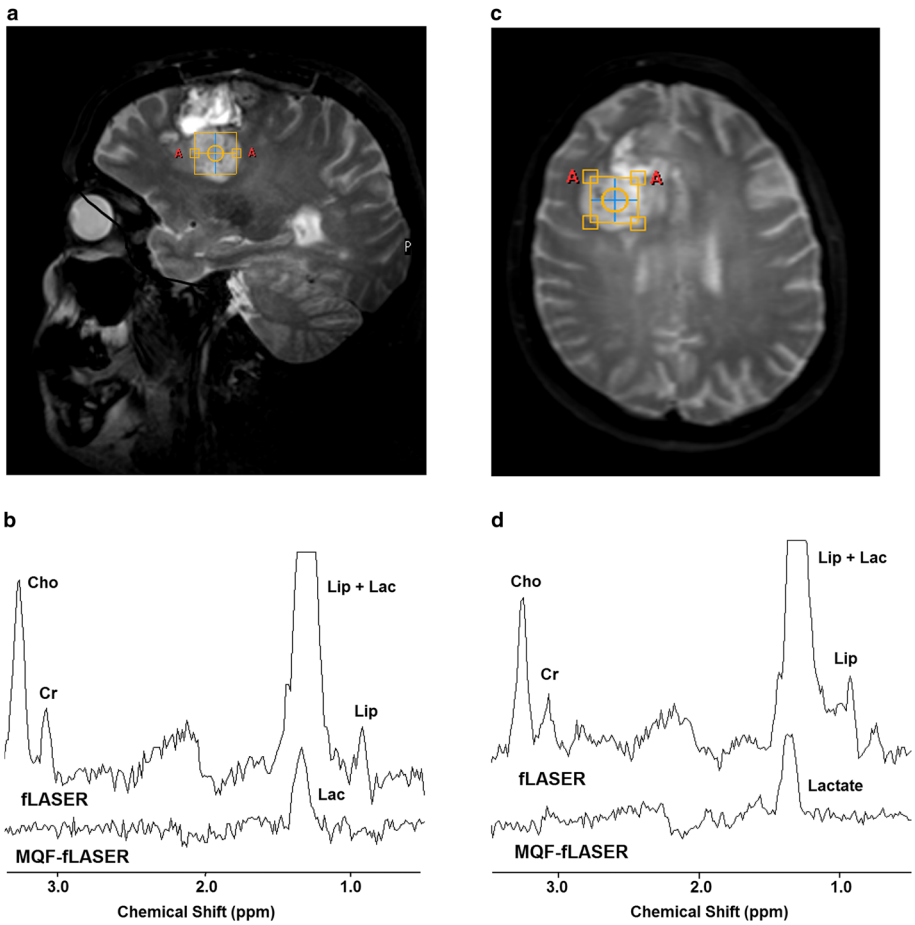

Figure 3. fLASER and MQF-fLASER spectra of high-grade brain tumours (glioblastoma multiforme). (a) Voxel location shown on sagittal T_1-weighted image (T_R/T_E = 11/4.6 ms). (b) Corresponding fLASER and MQF-fLASER spectra. Cho, choline; Cr, creatine; Lip, lipid; Lac, lactate. Water linewidth 6.0 Hz. (c) Voxel location shown on transverse T_2-weighted image (T_R/T_E = 2500/229 ms). (d) Corresponding fLASER and MQF-fLASER spectra, water linewidth 6.7 Hz. All spectra were acquired using T_R 1000 ms, T_E 144 ms, NSA 128 (fLASER) and 256 (MQF-fLASER), and voxel size $(2\ cm)^3$.

are in phase with the other resonances at this echo time of 144 ms. Lactate cannot be distinguished in these spectra. The MQF-fLASER spectra also show peaks at 1.3 ppm. These can be attributed to lactate, since lipid suppression to 0.86% reduces the lipid signals to well below the noise level. In several examples of brain tumours a peak was observed at 1.3 ppm in the fLASER spectra but not in the MQF-fLASER spectra, suggesting that these tumours contained lipid but not lactate. The concentrations of lactate were estimated assuming T_1 and T_2 of water were 1330 ms and 80 ms respectively (49), T_1 and T_2 of lactate were 1730 ms (50)and 453 ms (51) respectively, brain water concentration was 41 M (following Howe et al. (3)) and lactate selection

efficiency was 47% (based on the phantom measurement). This resulted in approximate lactate concentrations of 7.0 mM and 9.9 mM for the brain tumours shown in Fig. 3.

The MQF-fLASER spectrum of the large normal brain voxel (Fig. 4) reveals a broad peak centred at about 1.4 ppm with a width of about 20 Hz, and a sharper doublet to the right (centred at 1.35 ppm; splitting 7 Hz). The water linewidth in this voxel was 6.4 Hz. Given the repetition time used (2 s) it is more likely that the broad component arises from macromolecules rather than from lipids. The signal-to-noise ratio (peak height relative to rms noise) is about 12. Thus for the usual voxel size of approximately (2 cm)^3 the signal-to-noise ratio would be about unity, so not generally detectable. The corresponding peak in the spectrum without the MQF is approximately three times larger, showing that the selection efficiency of the MQF for this resonance is about 33%, which is nearly as high as for lactate. There are other

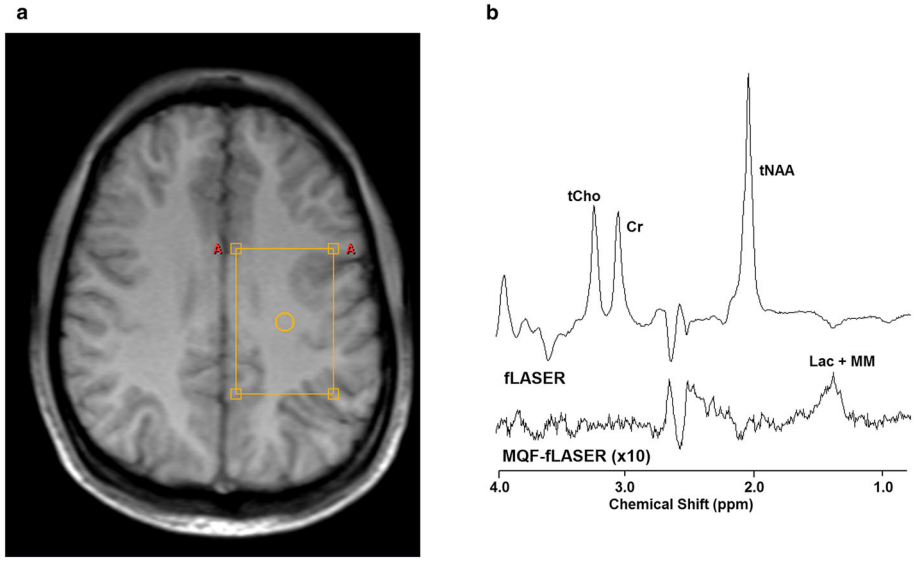

Figure 4. Example fLASER spectra from normal brain. (a) Voxel location shown on an axial T_1-weighted turbo field echo (TFE) image. (b) fLASER and MQF-fLASER spectra. tCho, total choline; Cr, creatine; tNAA, total N-acetyl aspartate; Lac, lactate MM, macromolecules. Voxel size 6 cm × 4 cm × 4 cm, T_R 2000 ms, T_E 144 ms, 4096 sample points over 4 kHz, NSA = 128 (fLASER) and 256 (MQF-fLASER). The water linewidth was 6.4 Hz.

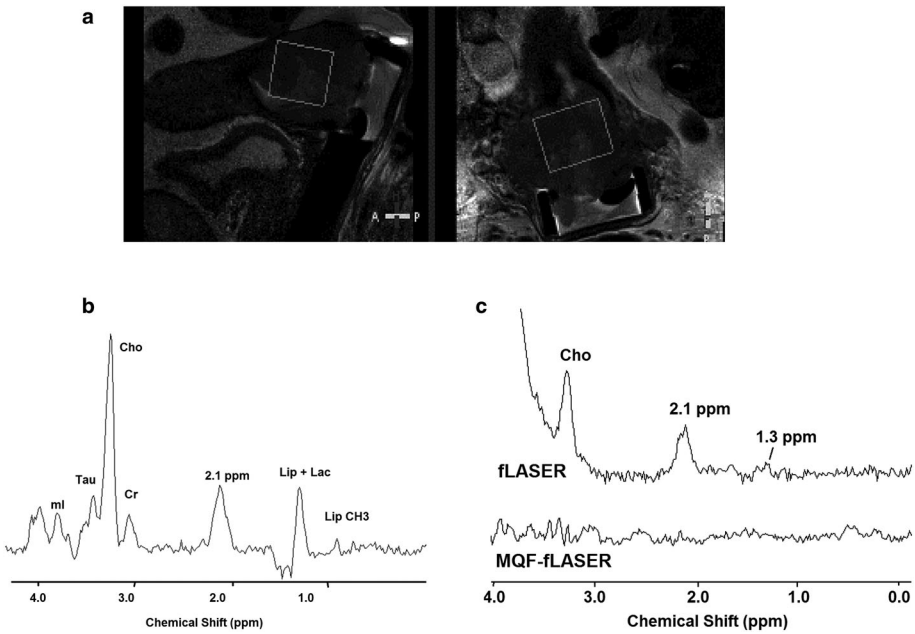

Figure 5. Example fLASER spectra from cervical tumours. (a) Voxel location shown on sagittal and coronal T_2-weighted images of Stage 2b cervical squamous cell carcinoma (T_R/T_E = 2750/80 ms). (b) Corresponding fLASER spectrum. mI, myo-inositol; Tau, taurine; Cho, choline; Cr, creatine; Lip, lipid; Lac, lactate. Voxel size 10 cm^3, T_R 1320 ms, T_E 144 ms, NSA 128, water linewidth 10 Hz. (c) Example fLASER and MQF-fLASER spectra from Stage 2b poorly differentiated squamous cell carcinoma. Note the very low levels of both lipid and lactate at 1.3 ppm in the fLASER spectrum, and the absence of any significant signals (including lactate) in the MQF-fLASER spectrum. Voxel 3.8 cm^3, T_R = 1346 ms, T_E = 144 ms, NSA = 128 (fLASER), 256 (MQF-fLASER), water line width 18 Hz.

NMR IN BIOMEDICINE

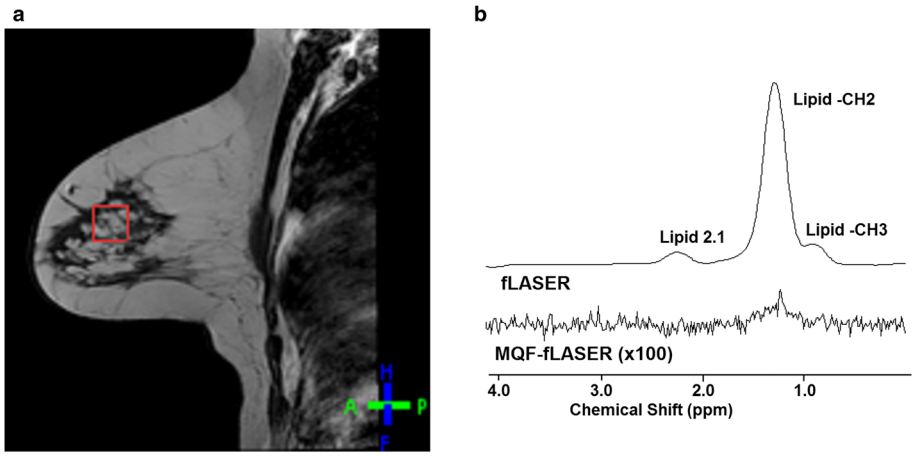

Figure 6. Example fLASER spectra from invasive lobular carcinoma. (a) Voxel position on sagittal T_1-weighted turbo spin echo (TSE) image (T_R/T_E = 399/10 ms). (b) Corresponding fLASER and MQF-fLASER spectra. Voxel size (2 cm)^3, T_R = 1000 ms, T_E = 144 ms, NSA = 128 (fLASER) and 256 (MQF-fLASER). Note the almost total elimination of the lipid peak at 1.3 ppm.

resonances visible in this MQF-fLASER spectrum of normal brain, in particular at about 2.5 ppm and 3.6 ppm. Since they are also seen in MQF-fLASER spectra from normal brain of other volunteers, they presumably arise from other metabolites or macromolecules not totally eliminated by the MQF. While these resonances have not been assigned, they are well resolved from the peaks at 1.3 ppm and therefore should not interfere with the measurements of lactate.

The fLASER spectra in cervix tumours (Fig. 5) are dominated by choline. There is a significant peak at 2.1 ppm that has been previously reported (source not yet identified (52,53)). The first example also shows well defined peaks from myo-inositol, taurine, and creatine. In spite of the presence of a peak at 1.3 ppm in the fLASER spectra of some cervix tumours, no MQF-fLASER spectra showed significant peaks at 1.3 ppm and hence did not detect any significant signals from lactate (Fig. 5(c)).

The fLASER spectrum from the breast lesion (Fig. 6(a)) is totally dominated by lipid. The peak at 1.3 ppm in the corresponding MQF-fLASER spectrum has an amplitude of 0.16% relative to that in Fig. 6(a). It is not possible to determine what proportions of this peak are due to lactate and lipid, but it demonstrates that lipid is largely eliminated by the filter.

DISCUSSION

The use of FOCI pulses permitted the implementation of a semi-LASER single-voxel MRS localization sequence compatible with a standard clinical MRI system transmitting with a body coil with limited B_1 amplitude. For the standard PRESS sequence, with RF bandwidths for the refocusing pulses of 1200 Hz, the chemical shift displacement between the lactate –CH and the lactate $–CH_3$ voxels is approximately 30% (in each direction), but by using the FOCI pulses with bandwidth of 12 kHz this was reduced to approximately 3%. The relative displacement of the acquired voxels from all metabolites at different chemical shifts was therefore also much reduced, while signals from the lactate multiplet were greatly increased owing to the large reduction in the chemical shift displacement effect (Fig. 2). Thus, even without the use of an MQF, the fLASER sequence is much to be preferred compared with standard PRESS sequences for the detection of lactate. The main limitation is the increased minimum values for T_E and T_R (76 ms and 1000 ms respectively in the current implementation) owing to the number and duration of the refocusing FOCI pulses. However, for detection of lactate these are not a restriction, since for a refocused lactate doublet one requires a T_E of 144 ms, and with a T_1 of about 1.73 s (50) the optimum signal-to-noise ratio is achieved for a repetition time of about 2.2 s.

The measurements in safflower oil demonstrated that in the current implementation the 1.3 ppm lipid peak is reduced to less than 1%. Further fat suppression is possible by incorporating longer spoiler gradient pulses, but at the expense of increasing the minimum echo time. The data from the breast tumour show that lipid is also effectively reduced under the conditions experienced *in vivo*. This shows that, if the peak at 1.3 ppm in the MQF-fLASER spectrum has a signal greater than 1% of the lipid in the corresponding non-filtered spectrum, it may be reasonably ascribed as predominantly arising from lactate.

Although incorporation of the MQF module into the fLASER sequence suppressed signals from singlets and retained lactate signals, the penalty for this single-shot approach was a reduction in lactate signal intensity by a little over 50%, which is admittedly a serious loss, especially when lactate concentrations are low. However, this still exceeded the signal from the standard PRESS sequence. Methods exist to recover the full signal of lactate, using either spin echo difference methods (29) or MQFs (32), but at the expense of introducing a phase cycle. In the brain this would probably be acceptable and lead to improved signal intensity, but for extra-cranial tumours, where there may be both increased lipid and motion, add–subtract schemes are best avoided.

A further limitation of the MQF scheme is that when no lactate signal is seen (for example in the cervical tumours) there is uncertainty as to whether this indicates that lactate concentrations are below the detection threshold, or whether one has had a technical failure. Acquisition of a few transients of the corresponding spectrum without the MQF or water suppression provides significant reassurance regarding technical aspects including shim quality and provides a water reference to aid quantification. Further acquisition of a water-suppressed spectrum will also provide complementary information regarding other MR-visible metabolites, but at the expense of extended measurement duration.

For the MQF-fLASER sequence specific absorption rate (SAR) was dominated by the FOCI pulses with only 1% added by the MQF pulses, yielding a minimum *T* of about 1 s (for a maximum SAR to the head of 3.2 W/kg). It was found that placing the MQF selection gradients at the magic angle (as previously recommended (42)) was definitely important to eliminate large near-resonant artefacts otherwise observed.

As with previous reports, lactate signals were detected in some but not all of the brain tumours studied. Although *in vivo* studies measuring lactate by direct detection in brain tumours have been generally confused by overlap with lipid peaks, they do suggest a large variation in lactate concentration, for example 11.7 ± 7.0 mM in glioblastomas (3). Measurements on tissue samples do not suffer the same problem of lipid overlap, although they are compromised by the rapid changes in lactate post-excision (54). However, these studies also suggest that there is a high degree of variation in lactate content between patients (55). The measurements in normal brain showed that, while the MQF is almost as good at selecting signals from the macromolecule peak near 1.3 ppm as it is in selecting lactate, for a standard voxel size of about $(2\ cm)^3$ this is unlikely to be detectable unless the signal from macromolecules is significantly elevated. When a good shim is achievable, any signals from macromolecules can often be discriminated from those of lactate on the basis of linewidth, and also on the basis of chemical shift (20); however, in some cases the contribution of macromolecules to the MQF-fLASER peak at 1.3 ppm cannot be totally excluded.

Despite good quality spectra in the majority of the cervix tumours studied (e.g. Fig. 5(b)), no lactate MQF signals were seen. In many cases this was consistent with the absence of a lactate + lipid peak at 1.3 ppm in the fLASER direct detection spectra, showing that these tumours had no significant content of either lactate or lipid. In the other cases the lipid content was eliminated by the MQF-fLASER sequence. The absence of significant amounts of lactate in cervical tumours was surprising, as these tumours are classically hypoxic. Although lactate signals have been reported in several *ex vivo* measurements of cervical tumour samples (56,57), these may reflect a different population of tumours, with a contribution from post-excision metabolism. A similar absence of significant lactate has recently been reported in prostate tumours, in which measurements at 3 T by Kobus *et al*. concluded that any lactate present must be below their detection threshold of about 1.5 mM (22).

CONCLUSION

fLASER and MQF-fLASER sequences have been implemented and demonstrated *in vitro* and *in vivo*. They are both effective at detecting lactate, while the MQF-fLASER sequence has the advantage of suppressing co-resonant signals from tissue lipids to less than 1%. Measurements in a pilot cohort of patients revealed lactate signals in some brain tumours but no significant lactate in any of the cervix tumours studied. Lipid was well suppressed in all cases. Use of these sequences should increase the potential of lactate measurements as a biomarker in targeted anti-cancer treatments as well as in measurements of tissue hypoxia.

Acknowledgements

We thank Dave Higgins and colleagues from Philips Clinical Science for provision and support of the sequence programming environment, and in particular for the LASER code, which was modified from a version written for their 7 T system. We also thank the research radiographers (Veronica Morgan, Sharon Giles, and Alison Macdonald) at the Royal Marsden Hospital for their assistance in acquiring the clinical scans.

We gratefully acknowledge funding from Cancer Research UK (project grant C7270/A13149), the CRUK and EPSRC Cancer Imaging Centre in association with the MRC and Department of Health (England) grants C1060/A10334 and C1060/A16464, and NHS funding to the NIHR Biomedical Research Centre and Clinical Research Facility. MOL is a NIHR senior investigator.

REFERENCES

1. Veech RL. The metabolism of lactate. NMR Biomed. 1991; 4(2): 53–58.
2. Oshiro S, Tsugu H, Komatsu F, Abe H, Onishi H, Ohmura T, Iwaasa M, Sakamoto S, Fukushima T. Quantitative assessment of gliomas by proton magnetic resonance spectroscopy. Anticancer Res 2007; 27(6A): 3757–3763.
3. Howe FA, Barton SJ, Cudlip SA, Stubbs M, Saunders DE, Murphy M, Wilkins P, Opstad KS, Doyle VL, McLean MA, Bell BA, Griffiths JR. Metabolic profiles of human brain tumors using quantitative in vivo ^{1}H magnetic resonance spectroscopy. Magn. Reson. Med. 2003; 49(2): 223–232.
4. Tessem MB, Swanson MG, Keshari KR, Albers MJ, Joun D, Tabatabai ZL, Simko JP, Shinohara K, Nelson SJ, Vigneron DB, Gribbestad IS, Kurhanewicz J. Evaluation of lactate and alanine as metabolic biomarkers of prostate cancer using ^{1}H HR-MAS spectroscopy of biopsy tissues. Magn. Reson. Med. 2008; 60(3): 510–516.
5. Bezabeh T, Odlum O, Nason R, Kerr P, Sutherland D, Patel R, Smith IC. Prediction of treatment response in head and neck cancer by magnetic resonance spectroscopy. Am. J. Neuroradiol. 2005; 26(8): 2108–2113.
6. Walenta S, Chau TV, Schroeder T, Lehr HA, Kunz-Schughart LA, Fuerst A, Mueller-Klieser W. Metabolic classification of human rectal adenocarcinomas: a novel guideline for clinical oncologists? J. Cancer Res. Clin. Oncol. 2003; 129(6): 321–326.
7. Schwickert G, Walenta S, Sundfor K, Rofstad EK, Mueller-Klieser W. Correlation of high lactate levels in human cervical cancer with incidence of metastasis. Cancer Res. 1995; 55(21): 4757–4759.
8. Walenta S, Salameh A, Lyng H, Evensen JF, Mitze M, Rofstad EK, Mueller-Klieser W. Correlation of high lactate levels in head and neck tumors with incidence of metastasis. Am. J. Pathol. 1997; 150(2): 409–415.
9. Walenta S, Wetterling M, Lehrke M, Schwickert G, Sundfor K, Rofstad EK, Mueller-Klieser W. High lactate levels predict likelihood of metastases, tumor recurrence, and restricted patient survival in human cervical cancers. Cancer Res. 2000; 60(4): 916–921.
10. Brizel DM, Schroeder T, Scher RL, Walenta S, Clough RW, Dewhirst MW, Mueller-Klieser W. Elevated tumor lactate concentrations predict for an increased risk of metastases in head-and-neck cancer. Int. J. Radiat. Oncol. Biol. Phys. 2001; 51(2): 349–353.
11. Huang MQ, Nelson DS, Pickup S, Qiao H, Delikatny EJ, Poptani H, Glickson JD. In vivo monitoring response to chemotherapy of human diffuse large B-cell lymphoma xenografts in SCID mice by ^{1}H and ^{31}P MRS. Acad. Radiol. 2007; 14(12): 1531–1539.
12. Ward CS, Venkatesh HS, Chaumeil MM, Brandes AH, Vancriekinge M, Dafni H, Sukumar S, Nelson SJ, Vigneron DB, Kurhanewicz J, James CD, Haas-Kogan DA, Ronen SM. Noninvasive detection of target modulation following phosphatidylinositol 3-kinase inhibition using hyperpolarized ^{13}C magnetic resonance spectroscopy. Cancer Res. 2010; 70(4): 1296–1305.
13. Chung Y-L, Troy H, Judson IR, Griffiths JR, Leach MO, Eykyn TR. Dichloroacetate treatment resulted in a dramatic drop in the conversion of hyperpolarised 1-13C labelled pyruvate to lactate in human colon carcinoma cells. Proceedings of the 18th Annual Meeting, ISMRM, Stockholm, Sweden, 2010; 4791.
14. Falck Miniotis M, Arunan V, Eykyn TR, Marais R, Workman P, Leach MO, Beloueche-Babari M. MEK1/2 inhibition decreases lactate in BRAF-driven human cancer cells. Cancer Res. 2013; 73(13): 4039–4049.

15. Semenza GL. Tumor metabolism: cancer cells give and take lactate. J. Clin. Invest. 2008; 118(12): 3835–3837.
16. McLean MA, Sun A, Bradstreet TE, Schaeffer AK, Liu H, Iannone R, Herman G, Railkar RA, Joubert I, Gillard JH, Price SJ, Griffiths JR. Repeatability of edited lactate and other metabolites in astrocytoma at 3T. J. Magn. Reson. Imaging 2012; 36(2): 468–475.
17. Park I, Chen AP, Zierhut ML, Ozturk-Isik E, Vigneron DB, Nelson SJ. Implementation of 3 T lactate-edited 3D 1H MR spectroscopic imaging with flyback echo-planar readout for gliomas patients. Ann. Biomed. Eng. 2011; 39(1): 193–204.
18. Deviers A, Ken S, Filleron T, Rowland B, Laruelo A, Catalaa I, Lubrano V, Celsis P, Berry I, Mogicato G, Cohen-Jonathan Moyal E, Laprie A. Evaluation of the lactate-to-*N*-acetyl-aspartate ratio defined with magnetic resonance spectroscopic imaging before radiation therapy as a new predictive marker of the site of relapse in patients with glioblastoma multiforme. Int. J. Radiat. Oncol. Biol. Phys. 2014; 90(2): 385–393.
19. Laprie A, Pirzkall A, Haas-Kogan DA, Cha S, Banerjee A, Le TP, Lu Y, Nelson S, McKnight TR. Longitudinal multivoxel MR spectroscopy study of pediatric diffuse brainstem gliomas treated with radiotherapy. Int. J. Radiat. Oncol. Biol. Phys. 2005; 62(1): 20–31.
20. Edden RA, Harris AD, Murphy K, Evans CJ, Saxena N, Hall JE, Bailey DM, Wise RG. Edited MRS is sensitive to changes in lactate concentration during inspiratory hypoxia. J. Magn. Reson. Imaging 2010; 32(2): 320–325.
21. Mellon EA, Lee SC, Pickup S, Kim S, Goldstein SC, Floyd TF, Poptani H, Delikatny EJ, Reddy R, Glickson JD. Detection of lactate with a Hadamard slice selected, selective multiple quantum coherence, chemical shift imaging sequence (HDMD-SelMQC-CSI) on a clinical MRI scanner: application to tumors and muscle ischemia. Magn. Reson. Med. 2009; 62(6): 1404–1413.
22. Kobus T, Wright AJ, Van Asten JJ, Heerschap A, Scheenen TW. In vivo ^{1}H MR spectroscopic imaging of aggressive prostate cancer: can we detect lactate? Magn. Reson. Med. 2014; 71(1): 26–34.
23. Kelley DA, Wald LL, Star-Lack JM. Lactate detection at 3T: compensating J coupling effects with BASING. J. Magn. Reson. Imaging 1999; 9(5): 732–737.
24. Edden RA, Schar M, Hillis AE, Barker PB. Optimized detection of lactate at high fields using inner volume saturation. Magn. Reson. Med. 2006; 56(4): 912–917.
25. Janich MA, Schulte RF, Schwaiger M, Glaser SJ. Robust slice-selective broadband refocusing pulses. J. Magn. Reson. 2011; 213(1): 126–135.
26. Charles-Edwards GD, Jan W, To M, Maxwell D, Keevil SF, Robinson R. Non-invasive detection and quantification of human foetal brain lactate *in utero* by magnetic resonance spectroscopy. Prenat. Diagn. 2010; 30(3): 260–266.
27. Star-Lack J, Spielman D, Adalsteinsson E, Kurhanewicz J, Terris DJ, Vigneron DB. In vivo lactate editing with simultaneous detection of choline, creatine, NAA, and lipid singlets at 1.5 T using PRESS excitation with applications to the study of brain and head and neck tumors. J. Magn. Reson. 1998; 133(2): 243–254.
28. Smith MA, Koutcher JA, Zakian KL. J-difference lactate editing at 3.0 Tesla in the presence of strong lipids. J. Magn. Reson. Imaging 2008; 28(6): 1492–1498.
29. Mescher M, Merkle H, Kirsch J, Garwood M, Gruetter R. Simultaneous *in vivo* spectral editing and water suppression. NMR Biomed. 1998; 11(6): 266–272.
30. Le QT, Koong A, Lieskovsky YY, Narasimhan B, Graves E, Pinto H, Brown JM, Spielman D. *In vivo* ^{1}H magnetic resonance spectroscopy of lactate in patients with stage IV head and neck squamous cell carcinoma. Int. J. Radiat. Oncol. Biol. Phys. 2008; 71(4): 1151–1157.
31. Trimble LA, Shen JF, Wilman AH, Allen PS. Lactate editing by means of selective pulse filtering of both zero- and double-quantum coherence signals. J. Magn. Reson. 1990; 86: 191–198.
32. He Q, Shungu DC, van Zijl PCM, Bhujwalla ZM, Glickson JD. Single-scan *in vivo* lactate editing with complete lipid and water suppression by selective mltiple-quantum-coherence transfer (Sel-MQC) with application to tumors. J. Magn. Reson. B 1995; 106: 203–211.
33. Harris LM, Tunariu N, Messiou C, Hughes J, Wallace T, deSouza NM, Leach MO, Payne GS. Evaluation of lactate detection using selective multiple quantum coherence in phantoms and brain tumours. NMR Biomed. 2015. DOI: 10.1002/nbm.3255
34. Lei H, Dunn J. The effects of slice-selective excitation/refocusing in localized spectral editing with gradient-selected double-quantum coherence transfer. J. Magn. Reson. 2001; 150(1): 17–25.
35. Ordidge RJ, Wylezinska M, Hugg JW, Butterworth E, Franconi F. Frequency offset corrected inversion (FOCI) pulses for use in localized spectroscopy. Magn. Reson. Med. 1996; 36(4): 562–566.
36. Payne GS, Leach MO. Implementation and evaluation of frequency offset corrected inversion (FOCI) pulses on a clinical MR system. Magn. Reson. Med. 1997; 38(5): 828–833.
37. Kinchesh P, Ordidge RJ. Spin-echo MRS in humans at high field: LASER localisation using FOCI pulses. J. Magn. Reson. 2005; 175(1): 30–43.
38. Andronesi OC, Ramadan S, Ratai EM, Jennings D, Mountford CE, Sorensen AG. Spectroscopic imaging with improved gradient modulated constant adiabaticity pulses on high-field clinical scanners. J. Magn. Reson. 2010; 203(2): 283–293.
39. Arteaga de Castro CS, Boer VO, Andreychenko A, Wijnen JP, van der Heide UA, Luijten PR, Klomp DW. Improved efficiency on editing MRS of lactate and gamma-aminobutyric acid by inclusion of frequency offset corrected inversion pulses at high fields. NMR Biomed. 2013; 26(10): 1213–1219.
40. Steinseifer IK, van Asten JJ, Weiland E, Scheenen TW, Maas MC, Heerschap A. Improved volume selective ^{1}H MR spectroscopic imaging of the prostate with gradient offset independent adiabaticity pulses at 3 tesla. Magn. Reson. Med. 2014.
41. Near J, Romagnoli C, Curtis AT, Klassen LM, Izawa J, Chin J, Bartha R. High-field MRSI of the prostate using a transmit/receive endorectal coil and gradient modulated adiabatic localization. J. Magn. Reson. Imaging 2009; 30(2): 335–343.
42. Thompson RB, Allen PS. Contamination of single-voxel multiple quantum filters by external water signals arising from intermolecular multiple quantum coherences. Magn. Reson. Med. 2009; 62(3): 796–801.
43. Naressi A, Couturier C, Devos JM, Janssen M, Mangeat C, de Beer R, Graveron-Demilly D. Java-based graphical user interface for the MRUI quantitation package. Magn. Reson. Mater. Phys. Biol. Med. 2001; 12(2/3): 141–152.
44. Ratiney H, Coenradie Y, Cavassila S, van Ormondt D, Graveron-Demilly D. Time-domain quantitation of 1H short echo-time signals: background accommodation. Magn. Reson. Mater. Phys. Biol. Med. 2004; 16(6): 284–296.
45. Ratiney H, Sdika M, Coenradie Y, Cavassila S, van Ormondt D, Graveron-Demilly D. Time-domain semi-parametric estimation based on a metabolite basis set. NMR Biomed. 2005; 18(1): 1–13.
46. Gilderdale DJ, deSouza NM, Coutts GA, Chui MK, Larkman DJ, Williams AD, Young IR. Design and use of internal receiver coils for magnetic resonance imaging. Br. J. Radiol. 1999; 72(864): 1141–1151.
47. Behar KL, Rothman DL, Spencer DD, Petroff OA. Analysis of macromolecule resonances in ^{1}H NMR spectra of human brain. Magn. Reson. Med. 1994; 32(3): 294–302.
48. He Q, Shungu DC, van Zijl PC, Bhujwalla ZM, Glickson JD. Single-scan *in vivo* lactate editing with complete lipid and water suppression by selective multiple-quantum-coherence transfer (Sel-MQC) with application to tumors. J. Magn. Reson. B 1995; 106(3): 203–211.
49. Wansapura JP, Holland SK, Dunn RS, Ball WS, Jr. NMR relaxation times in the human brain at 3.0 tesla. J. Magn. Reson. Imaging 1999; 9(4): 531–538.
50. Terpstra M, High WB, Luo Y, de Graaf RA, Merkle H, Garwood M. Relationships among lactate concentration, blood flow and histopathologic profiles in rat C6 glioma. NMR Biomed. 1996; 9(5): 185–194.
51. Matsumura A, Isobe T, Takano S, Kawamura H, Anno I. Non-invasive quantification of lactate by proton MR spectroscopy and its clinical applications. Clin. Neurol. Neurosurg. 2005; 107(5): 379–384.
52. Mahon MM, Cox IJ, Dina R, Soutter WP, McIndoe GA, Williams AD, deSouza NM. ^{1}H magnetic resonance spectroscopy of preinvasive and invasive cervical cancer: in vivo–ex vivo profiles and effect of tumor load. J. Magn. Reson. Imaging 2004; 19(3): 356–364.
53. De Silva SS, Payne GS, Morgan VA, Ind TE, Shepherd JH, Barton DP, deSouza NM. Epithelial and stromal metabolite changes in the transition from cervical intraepithelial neoplasia to cervical cancer: an in vivo 1H magnetic resonance spectroscopic imaging study with ex vivo correlation. Eur. Radiol. 2009; 19(8): 2041–2048.
54. Opstad KS, Bell BA, Griffiths JR, Howe FA. An assessment of the effects of sample ischaemia and spinning time on the metabolic profile of brain tumour biopsy specimens as determined by high-resolution magic angle spinning ^{1}H NMR. NMR Biomed. 2008; 21(10): 1138–1147.

55. Martinez-Bisbal MC, Marti-Bonmati L, Piquer J, Revert A, Ferrer P, Llacer JL, Piotto M, Assemat O, Celda B. ^{1}H and ^{13}C HR-MAS spectroscopy of intact biopsy samples *ex vivo* and *in vivo* ^{1}H MRS study of human high grade gliomas. NMR Biomed. 2004; 17(4): 191–205.
56. Sitter B, Bathen T, Hagen B, Arentz C, Skjeldestad FE, Gribbestad IS. Cervical cancer tissue characterized by high-resolution magic angle spinning MR spectroscopy. Magn. Reson. Mater. Phys. Biol. Med. 2004; 16(4): 174–181.
57. De Silva SS, Payne GS, Thomas V, Carter PG, Ind TE, deSouza NM. Investigation of metabolite changes in the transition from pre-invasive to invasive cervical cancer measured using ^{1}H and ^{31}P magic angle spinning MRS of intact tissue. NMR Biomed. 2009; 22(2): 191–198.